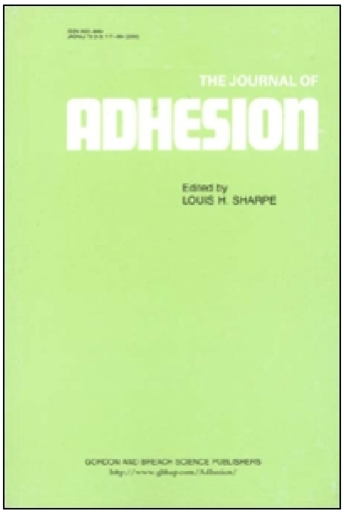

The Journal of Adhesion
Publication details, including instructions for authors and subscription information:
http://www.informaworld.com/smpp/title~content=t713453635

Interfacial Friction in Filled Polymers Initiated by Adhesive Debonding. III. Physical Modelling

V. V. Moshev[a]; V. N. Kovrov[a]
[a] Institute of Continuous Media Mechanics, Russian Academy of Sciences, Perm, Russia

To cite this Article Moshev, V. V. and Kovrov, V. N.(1998) 'Interfacial Friction in Filled Polymers Initiated by Adhesive Debonding. III. Physical Modelling', The Journal of Adhesion, 65: 1, 91 — 103
To link to this Article: DOI: 10.1080/00218469808012240
URL: http://dx.doi.org/10.1080/00218469808012240

J. Adhesion, 1998, Vol. 65, pp. 91–103
Reprints available directly from the publisher
Photocopying permitted by license only

Interfacial Friction in Filled Polymers Initiated by Adhesive Debonding. III. Physical Modelling

V. V. MOSHEV and V. N. KOVROV

Institute of Continuous Media Mechanics, Russian Academy of Sciences, Perm', 614061, Russia

(Received 19 April 1996; In final form 6 March 1997)

Interfacial friction as a dissipative mechanism in particulate composites is investigated by means of two modelling devices. The specific friction as a function of the clamping pressure and loading rate for a rubber-steel piston pair has been investigated and a corresponding empirical relationship has been derived therefrom. The resulting relationships show promise for simulating frictional manifestations in the framework of debonded particle-reinforced polymer matrix composites.

Keywords: Physical modelling of interfacial friction; time-dependent friction; frictional stress relaxation; rubber; hysteresis; damaged particulate-filled polymer composite

1. INTRODUCTION

Recently, some experimental data have been reported characterizing the dissipative peculiarities observed in damaged particulate composites [1, 2]. It was demonstrated that the adhesive debonding gives rise to a specific dissipation mechanisms of the Coulomb friction type between contacting debonded interfaces. To make this frictional effect more pronounced, care was taken to exclude the proper visco-elasticity of the matrix phase. To do this, a highly-plasticized rubbery material with no discernible intrinsic dissipation was used [1].

Interface friction in the form of pronounced hysteresis loops initiated by adhesive debonding was observed, the hysteresis loops being strongly broadened under moderate superimposed pressures [1].

Moreover, the existence of the stress relaxation mechanism originated exclusively by the interfacial friction was demonstrated experimentally in [2], where the debonded composites based on a non-dissipative matrix were tested. The rate of stress relaxation, as well, has manifested itself as a pressure-sensitive process.

The interfacial friction dissipation in particulate composites as such needs further clarification directed to obtaining a quantitative description of this phenomenon. Most likely, this could be achieved through the creation of physical models capturing its essential features on a macroscale level. According to this paradigm, several modelling devices have been designed and tested. This paper describes the outcomes of this work.

2. THEORETICAL BACKGROUND

Generalities concerning the dependence of the frictional force of rubber on pressure and rate of sliding are known [3–5]: frictional resistance increases with pressure and rate of sliding. However, it manifests itself in a variety of specific conditions. Some of them represent a fixed rubber surface sliding along a solid surface as, for example, in Reference [3]. Others, on the contrary, are situations where a solid body slides along the rubber surface, being partly indented into a soft rubbery phase (the so-called Schallamach waves [4]). The friction phenomenon under consideration in the present work is essentially different from the situations indicated above. It represents a discontinuous process, closed on a microscale level around scattered filler particles embedded in a continuous matrix. Friction appears only after microdamage has occurred in the form of interfacial debonding between the filler particles and the matrix as shown in Figure 1. The cell is assumed to have the form of an elastic cylinder (matrix) with a rigid spherical inclusion (filler particle) placed at its center. The suitability of this choice is justified elsewhere [5]. During extension of the cell, the debonded matrix slips along the inclusion at the equatorial zone, where the interface contact is retained continuously. This contact zone is the source of the friction. The rate of matrix slip along the filler surface cannot be uniform due to the geometrical and loading symmetry of the cell: it is zero at the equator and increases up to the separation line, where the matrix detaches from the inclusion. Figure 1 suggests, as well, that contact pressure along the sliding zone might also vary from some maximum value at the equator to zero at the line of separation.

We could not find appropriate data in the available literature for carrying out relevant calculations. The need for special-purpose experimentation was keenly felt.

Obviously, the complicated pattern of the actual frictional process cannot be accurately reproduced in an experimental facility capable of controlling the actual displacement and pressure distributions along the friction zone. Thus, simplified devices were constructed to provide insight into this phenomenon. This paper presents the results of such an experimental research.

3. EXPERIMENTAL DETAILS AND RESULTS

Two facilities have been designed and tested. The scheme of the first one, reflecting some important features of the friction phenomena, is shown in Figure 2. It represents a commercial rubber tube (1) placed over a steel piston (2), the left end of the tube being fixed to the piston while the right end is free to slide over the piston's surface. The free end is fixed on a hub (3) that is free to move along the piston. The left end of the piston and the right end of the hub are fixed in the clamps of a standard testing machine.

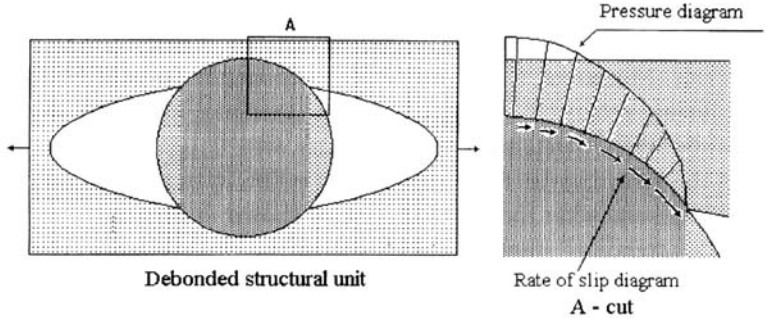

FIGURE 1 Scheme of the interface slipping inside the structural element.

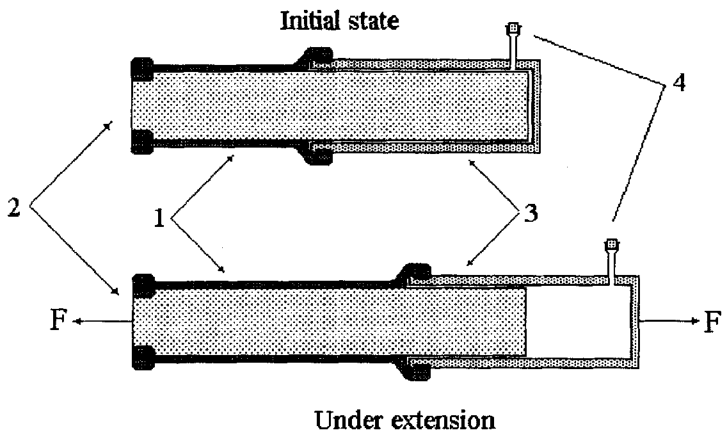

FIGURE 2 Sketch of the device for modelling structural rubber friction.

The experimental procedure consisted in extension of this assembly while recording both load and displacement. The tube has been labeled to follow the longitudinal strain distributions along the length of the tube. A void appears between the ends of the hub and piston simulating vacuole formation in particulate composites. Evidently the resistance of the device to extension results from both the stiffness of the rubber tube and the frictional drag between the rubber tube and the piston rod. The vacuum void originates during initial loading, while atmospheric pressure clamps the tube tightly against the piston, providing a normal force for the friction that is to be investigated.

Figure 3a illustrates typical strain distributions along the piston with increasing displacement. Each strain state is recorded 10 minutes after the current stretch has been imposed to allow for relaxation. The presence of friction makes the longitudinal strain distribution strongly nonlinear. Moreover, a portion of the tube length remains undisturbed during extension which marks the existence of static friction. Evidently, the unstretched length shortens with elongation. The strain along the piston varies from the starting point, *a*, to the pull-point, *b*, modelling somewhat the slipping pattern shown in Figure 1.

The existence of static friction leads to the origination of residual strains when the applied load is released. Figure 3b depicts the strain distribution along the rubber tube after the force has dropped to zero during retraction.

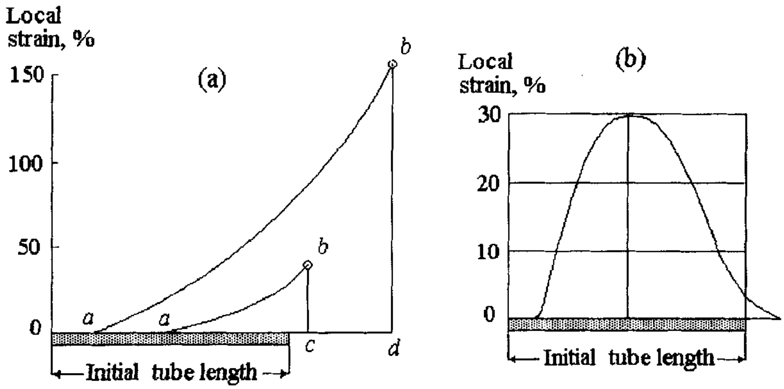

FIGURE 3 Local strain distribution along the rubber tube: (a) during sliding; (b) after retraction.

It has been observed that, after rapid extensions to a given stretch, the strain distribution evolves over time (Fig. 4a). A redistribution of local strains immediately after the stretch has been fixed leads to their partial diminution in the most-strained region at the expense of a negligible increase in the weakly-strained regions. A corresponding drop in the overall extension effort accompanies this process (Fig. 4b).

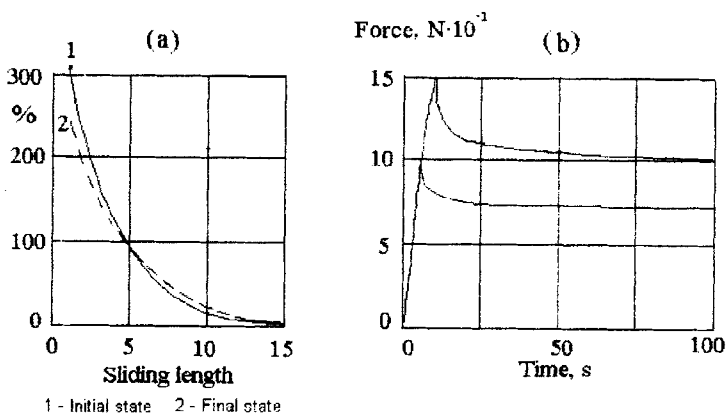

FIGURE 4 Local strain distribution and its change due to frictional slipping (a), and typical stress relaxation accompanying this process (b).

This observation indicates that time-dependent frictional shifts contribute to stress relaxation. Therefore, time-dependent friction cannot be ignored in structural modelling.

Usually, the frictional relaxation comes about together with other dissipative mechanisms such as, for instance, the matrix viscoelasticity. Their relative contribution depends on the properties of the constituent elements, the set-up geometry and the loading conditions. In our experiments, the proper dissipative ability of the tube might be reckoned as negligible. This can be seen from Figure 5. In the first experiment, the tube was extended at the rate of 20 mm/min to a stretch of 30 mm in the free state and then held to record the relaxation drop (curve 1). The second experiment was performed in the same manner, but with the tube put on the piston (curve 2), It is clearly seen that the relaxation drop with frictional participation is much greater than that characteristic of a free tube. So, in this example, the role of friction in the stress relaxation is considerable.

Evidently, the facility described above, while providing important qualitative results, is unsuitable for obtaining the quantitative relationships needed for numerical simulation. To attain the latter aim,

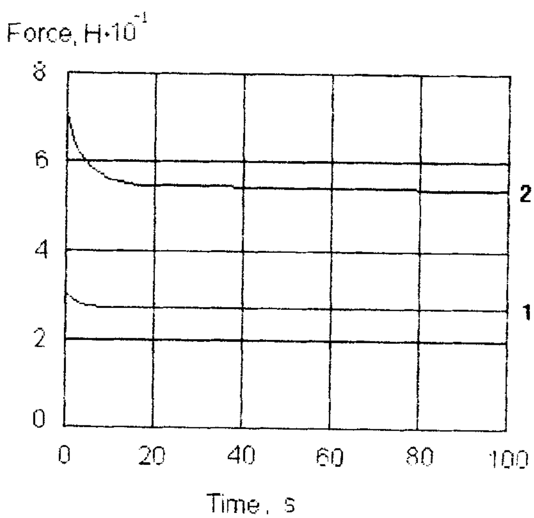

FIGURE 5 Comparison of the relaxation curves for dragged and free tubes: (1) frictionless case; (2) in the presence of friction.

another device has been developed and utilized. Its schematic diagram is shown in Figure 6. The main working parts are a thick-walled rubber hub, 1, fitted freely on a steel shaft, 2. This hub is fixed within a steel chamber, 3, designed for applying elevated pressure. It is covered by an antibuckling protective perforated shell, 4. The frictional resistance is obtained by drawing the shaft through the rubber hub under various pressures and rates of sliding. The geometry of the facility ensures a definite area of frictional contact. A load cell of the testing machine registers the frictional effort during drawing of the shaft through the hub at the imposed rate. The gauge, 5, connected with the chamber, records the imposed pressure level. Assuming incompressibility of the rubber hub and the absence of considerable clearance between the hub and the shaft, one may presume that the pressure of the hub on the shaft is equal to that of the gas inside the chamber.

The basic parameters of the facility and operating conditions were as follows: the diameter of the shaft, $d = 10\,\mathrm{mm}$; the contact length, $l = 40\,\mathrm{mm}$; the rates of sliding, $v = 0.1$, 1, 10, and 100 mm/s; pressures, $p = 0.1, 0.2, 0.3, 0.4$, and 0.5 MPa.

A plasticized butadiene-styrene rubber having a Young's modulus equal to 0.15 MPa was chosen for experimentation. This magnitude allowed the covering of the range of the friction *vs.* pressure sensitivity

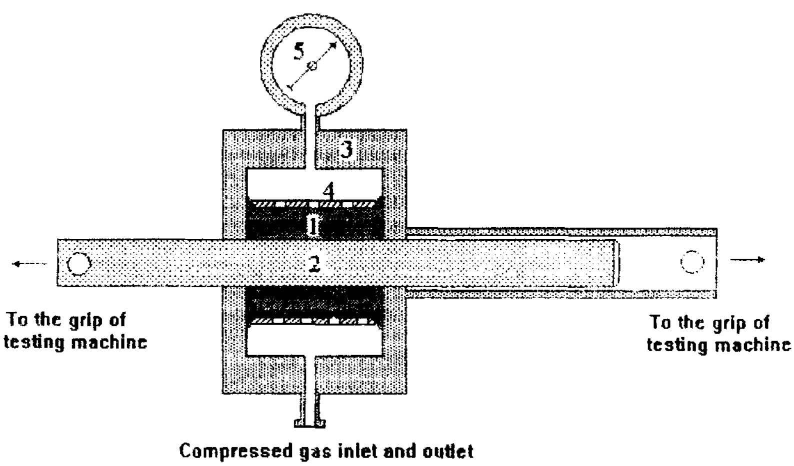

FIGURE 6 Scheme of the device for determination of the friction dependency on pressure and rate of sliding.

to a sufficient completeness within the limits of moderate values of p indicated above. The frictional force is represented in MPa.

The results of testing are presented in Figure 7. Here, the friction, f, means a specific magnitude, *i.e.*, the tangential stress in MPa. It is seen that both the pressure and the rate of sliding affect friction in a markedly non-linear manner. As a function of pressure, the friction increases from zero (or almost zero) at zero pressure to some limiting value characteristic of the given rate of slip. The f *versus* p dependence at vanishing rates may be considered as the dependence of the static friction on the pressure.

The rate-dependence of the friction is strongly non-linear, a tenfold increase in the rate of slip giving, on average, only about a 20% increase in the frictional force.

An empirical formula fit to the experimental data is given by:

$$f = 0.054(1 - \exp(-8.0p))(1 + 0.93\,v^{0.15}) \quad (1)$$

where f is the specific friction force defined as indicated above, p is the pressure on the contact surface in MPa, and v is the rate of sliding in mm/min.

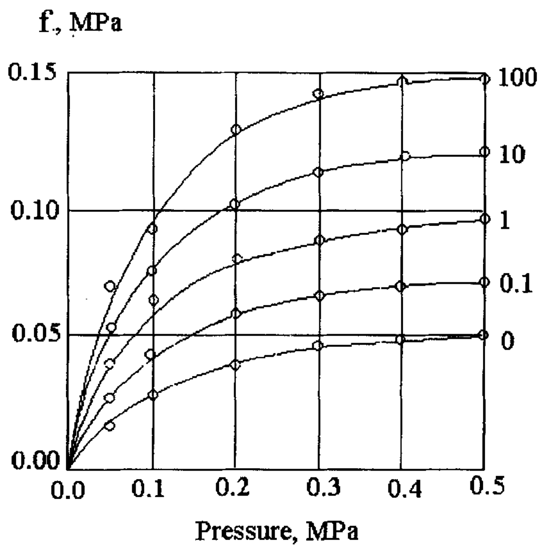

FIGURE 7 Dependence of the specific friction on pressure and rate of sliding in mm/min (indicated near the curves).

The results obtained clearly illustrate that friction in the system under consideration cannot be modelled according to the usual notion of the friction coefficient as a material property relating loads with frictional forces.

4. DISCUSSION

The data presented above provide insight (now at a qualitative level) into the manner in which the interfacial friction can affect the mechanical behavior of structural cells. Though they have been derived from a particular frictional pair, it is felt that (as far as it concerns frictional effects) the basic features are valid for other objects consisting of visco-elastic elements and solid substrates. This assumption provides a method for constructing simple mathematical models for a semiquantitative analysis.

Returning to the sketch in Figure 2, we model this physical object as a linear elastic spring resting on a substrate that resists the spring's extension (Fig. 8). Let the elastic stiffness of the spring be G. The left ends both of the spring and of the substrate are held together and fixed. The right end of the spring is extended along the substrate. It is assumed that the spring is applied to the substrate with a constant,

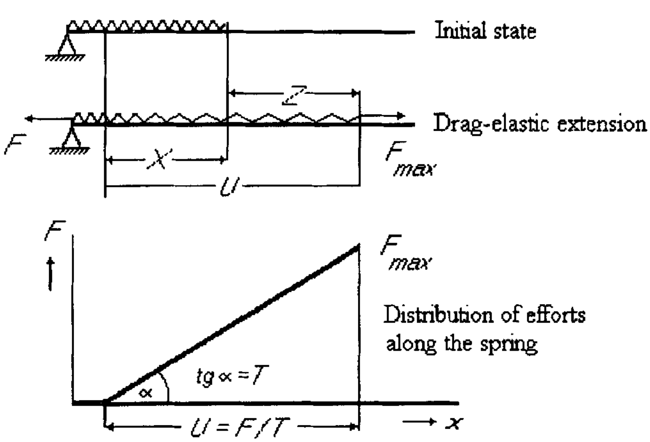

FIGURE 8 Drag-elastic motion modelling.

uniformly distributed pressure providing a constant specific (for a unit length) frictional force, T, along the moving length of the spring. The rate of extension is very low, permitting us to consider the friction force, T, as a constant value close to the static friction corresponding to the applied pressure, P.

The task is to estimate how the pulling force, F, depends on the displacement, Z, of the right end of the spring. In the framework of the adopted conditions, the sliding of the spring along the length of du on the substrate appears, when the difference in pulling effort, dF, at the ends of the element, du, becomes equal to the dragging resistance of the substrate, Tdu,

$$dF = Tdu. \tag{2}$$

Hence, a linear increase in F with respect to u along the slipping part of the spring can be postulated

$$F(u) = T(u - u_0), \tag{3}$$

where u_0 is the abscissa of the point at which spring slip appears.

The extension of the spring corresponding to a current force, F, within the sliding element, du, is obviously equal to F/G. It follows herefrom that the initial length, dx, of the strained element with a stretched length, du, can be expressed as

$$dx = du/(1 + F/G) \tag{4}$$

The expressions (3)–(4) are basic in computing tensile curves for systems with constant values of T. After simple intermediate mathematical manipulations, one arrives at a relation between the pulling force, F, applied to the end of the spring, and the end-displacement, Z, having the form (for the conditions of Figure 8)

$$Z = F/T - (G/T)\ln(1 + F/G). \tag{5}$$

This expression allows one to get the general idea of the influence of friction on the mechanical behavior of the system under consideration.

Figure 9 represents the dependence of tensile curves on the T/G ratio. It is seen that friction contributes significantly to the resistance of the model when T exceeds about 0.1 of G. At lesser values of T it may be practically neglected. This simple model explains well the increasing importance of friction with filler volume fraction. From Figure 1, it follows that the thickness of the matrix belt in the equatorial zone (A-zone) defines, in essence, the stiffness of the debonded cells. This matrix belt thickness decreases significantly with an increase in the filler volume fraction, while friction might not be influenced therewith. Therefore, the ratio of the friction magnitude to that of the cell stiffness should increase markedly with filler loading, which must enhance dissipative manifestations. That is actually the case. The experimental data presented in Figure 10 are extracted from Reference 1. They demonstrate a significant increase in hysteresis with increasing filler concentration for previously-debonded composite samples.

Eq. (1) (for plasticized butadiene-styrene rubber) has been used for calculating rate-dependent drag-elastic curves for the geometry of the model presented in Figure 2. Various rates of extension have been applied to the right end of the spring under uniformly applied pressure and tensile curves have been calculated. The calculated results are

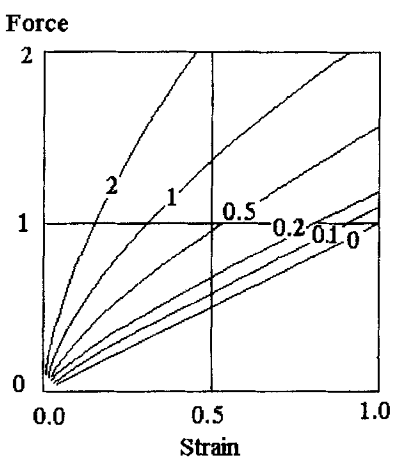

FIGURE 9 Influence of friction on tensile curves. Numbers on the curves designate T/G ratios.

displayed in Figure 11a, while in Figure 11b the experimental data obtained on a commercial rubber tube are presented as well. Qualitatively, the prediction agree well with experimental results.

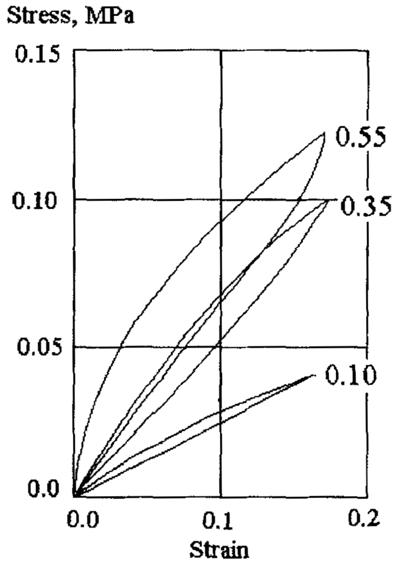

FIGURE 10 Hysteresis loops of the debonded specimens with different volume loadings indicated near the curves.

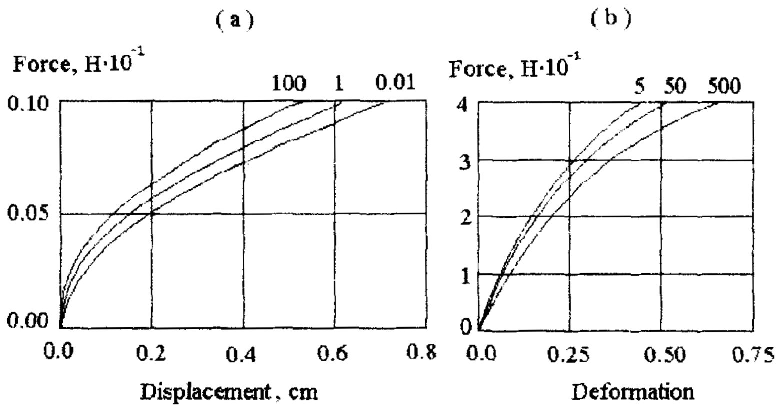

FIGURE 11 Comparison of the computed (a) and experimental (b) tensile curves at various rates of extension. Rates in mm/min are indicated near the curves.

The results reported provide evidence to support using the general form of Eq. (1) in structural investigations complicated by drag-elastic phenomena.

5. CONCLUSIONS

1. Two models have been presented for physical modelling of the effects of interfacial friction inside a damaged particulate polymer matrix composite.
2. Some general results characterizing the pressure and time dependence of the interface friction have been obtained with the first model. The specific friction as a function of the pressure and the rate of slipping for a rubber-steel piston pair has been investigated and the corresponding empirical relationship has been derived therefrom. It has been demonstrated that, in this case, the coefficient of friction is not material property.
3. Comparison with experiment has shown that these simple models are promising for the numerical simulation of particulate composites: for example, in the description of frictional dissipation in the framework of debonded structural cells of particulate composites.

Acknowledgements

The research reported in this paper has been supported by the Russian Academy of Sciences under Grant 94-01-00465-a.

References

[1] Moshev, V. V., "Interfacial friction in filled polymers initiated by adhesive debonding," *J. Adhesion* **35**, 181–186 (1991).
[2] Moshev, V. V., Kovrov, V. N. and Sannikov, L. S., "Interfacial friction in filled polymers initiated by adhesive debonding. II. Relaxation studies," *J. Adhesion* **43**, 239–243 (1993).
[3] Grosch, K. A., "The relation between the friction and visco-elastic properties of rubber," *J. Roy. Soc.* **274**, 21–39 (1963).
[4] Schallamach, A., in *The Physical of Tire Traction*, Ed. (Plenum Press, New York, 1974), p. 167.
[5] Moshev, V. V. and Kozhevnikova, L. L., "Unit cell evolution in structurally damageable particulate-filled elastomeric composites under simple extension," *J. Adhesion* **55**, 209–219 (1995).